Neutron Compton scattering investigation of sodium hydride: From bulk material to encapsulated nanoparticulates in amorphous silica gel

A. G. Seel,[1] A. Sartbaeva,[1] J. Mayers,[2] A. J. Ramirez-Cuesta,[2] and P. P. Edwards[1,a)]

[1]*Department of Chemistry, Inorganic Chemistry Laboratory, University of Oxford, South Parks Road, Oxford OX1 3QR, United Kingdom*
[2]*ISIS Facility, Rutherford Appleton Laboratory, Chilton, Didcot, Oxon OX11 0QX, United Kingdom*

In this study we utilize neutron Compton scattering (NCS) to determine differences in nuclear momentum distributions in NaH, both as bulk material and encapsulated as nanoscale particles (from 20 to 50 nm in diameter) within an amorphous silica-gel matrix (SiGNaH). In addition, elemental Na dispersed in such a matrix is also studied (SiGNa). Data treatment and fitting of experimental spectra yields comparison of the nuclear Compton profiles and radial momentum distributions for the proton in both bulk NaH and nanoscale SiGNaH, with resultant proton kinetic energies being in agreement with previous inelastic neutron studies of bulk NaH. Slight differences in proton radial momentum distributions for bulk and nanoscale systems are witnessed and discussed. The technique of stoichiometric-fixing is applied to the backscattering spectra of each system in order to examine changes in the Na profile width, and NCS is shown to be sensitive to the chemical environment change of this heavier nucleus. Examination of the Si and O profile widths in the gel samples also supports this method. © *2011 American Institute of Physics*. [doi:10.1063/1.3561493]

I. INTRODUCTION

Neutron Compton scattering (NCS), also referred to as deep inelastic neutron scattering (DINS), is a technique developed to probe the nuclear momentum distributions in condensed matter. Since the development of pulsed spallation neutron sources, the NCS spectrometers VESUVIO (Ref. 1) and its predecessor EVS at the ISIS facility (Rutherford Appleton Laboratories, UK) have utilized epithermal neutrons of the order of several tens of eVs to gather information on nuclear momentum distributions in a variety of light-atom-containing systems. While most of these systems are perhaps of greatest interest to the condensed-matter physicist, such as H_2/D_2 and H_2O/D_2O mixtures,[2,3] H_2O confinement[4,5] or elemental states,[6–8] systems of more direct relevance to chemistry have only recently been investigated. These include molecular compounds such as $(NH_3)_4$ $PdCl_6$ (Ref. 9) and $NaHF_2$,[10] systems containing strong hydrogen bonds,[11,12] biological systems,[13,14] Li-intercalated materials,[15] and some metal hydrides of the s-, d-, and f-blocks.[16,17]

As part of a wider investigation of NCS to systems of both chemical and physical interest, we present here NCS data on three systems: NaH in bulk, amorphous Na dispersed within an amorphous silica gel framework (SiGNa), and on its hydride product (SiGNaH) whereby the resulting NaH exists as nanoparticulates located within the gel. NaH is a powerful reducing agent with extensive application in synthetic organic chemistry, and recently the formation of SiGNaH was reported by Sartbaeva *et al.* as a potentially less pyrophoric and less air-sensitive source of NaH.[18] Here we begin by presenting a brief background to the theory of NCS followed by a discussion of data analysis for the systems being studied. Results are then presented for the three systems, examining the proton momentum distributions, proton Compton profiles, and mean kinetic energies. Profile widths for the Na, Si, and O species in each system are also detailed, with discussion of the application of NCS to heavier, mixed-mass systems.

Before detailing this study, two properties of NCS are worth discussing. The first is the great interest and speculation pertaining to the so-called "anomalous cross-section" for protons in NCS.[2,19–21] Considerable effort has gone into proving this effect to be real, and theorizing as to why it occurs. Needless to say this property has bearing on this study, where protons are present in two samples, but of all import is that this anomaly does not affect the measured widths of proton momentum distributions. Second, in some cases NCS has been used to look beyond the analysis of nuclear momentum distributions but go on to use those of the proton to reconstruct the Born–Oppenheimer potential experienced by the proton.[10,22] While not directly part of this work, it is worth noting as an exciting possibility in chemical physics, and the reader is referred to Ref. 10 for both an in depth discussion of this problem, and the application of NCS as a molecular probe in general.

II. THEORY OF NCS

The theory of neutron scattering and that of NCS can be found in a number of sources,[23–25] with only that relevant for understanding and interpretation of results in this study being presented here. The dynamic structure factor (also called the scattering law) for a neutron scattered from a collection of

a)Electronic mail: peter.edwards@chem.ox.ac.uk.

nuclei j, at an energy transfer ω and momentum transfer $\mathbf{q}$ is given by[26]

$$S(\mathbf{q}, \omega) = \frac{1}{2\pi \hbar N} \int_{-\infty}^{\infty} \exp(-i\omega t) \sum_{jj'} I_{jj'}(\mathbf{q}, t) \, dt, \qquad (1)$$

where

$$I_{jj'}(\mathbf{q}, t) = \langle \exp\{-i\mathbf{q} \cdot \hat{\mathbf{R}}_j(0)\} \exp\{i\mathbf{q} \cdot \hat{\mathbf{R}}_{j'}(t)\} \rangle. \qquad (2)$$

$\hat{\mathbf{R}}_j$ is the position operator for nucleus j, and the brackets $\langle \ldots \rangle$ denote a thermal average across the system. The leading approximation in NCS is the impulse approximation, which states

$$\hat{\mathbf{R}}_{j'}(t) = \hat{\mathbf{R}}_{j'}(0) + \frac{t}{M_{j'}} \hat{\mathbf{p}}_{j'}. \qquad (3)$$

$\hat{\mathbf{p}}_{j'}$ is defined as the momentum operator conjugate to $\hat{\mathbf{R}}_{j'}$, and M is the nuclear mass. It is also assumed that under the conditions of NCS all scattering is incoherent in nature, i.e., that $j = j'$. This is due to the wavelength of the incident neutrons being comparable to random displacements of the atoms from their mean positions (due to zero point motion or thermal effects) and thus coherent scattering averages to zero. Hence, the double sum in Eq. (1) reduces to

$$S(\mathbf{q}, \omega) = \frac{1}{2\pi \hbar N} \int_{-\infty}^{\infty} \exp(-i\omega t) \sum_{j} \langle \exp\{-i\mathbf{q} \cdot \hat{\mathbf{R}}_j(0)\}$$

$$\times \exp\{i\mathbf{q} \cdot \hat{\mathbf{R}}_j(0) + \frac{it}{M_j}\mathbf{q} \cdot \hat{\mathbf{p}}_j\} \rangle \, dt. \qquad (4)$$

Following standard treatment it is possible to show that the dynamic structure factor adopts the form of that of a free particle of mass M, with momentum distribution $n(\mathbf{p})$,[26]

$$S(\mathbf{q}, \omega) = \int_{-\infty}^{\infty} n(\mathbf{p})\delta \left(\omega - \frac{(\mathbf{p} + \mathbf{q})^2}{2M} + \frac{p^2}{2M} \right) \, d\mathbf{p}$$

$$= \frac{M}{q} J_M(y_M, \hat{\mathbf{q}}), \qquad (5)$$

where

$$J_M(y_M, \hat{\mathbf{q}}) = \int_{-\infty}^{\infty} n(\mathbf{p})\delta(y_M - \mathbf{p} \cdot \hat{\mathbf{q}}) \, d\mathbf{p} \qquad (6)$$

and

$$y_M = \frac{M}{q} \left(\omega - \frac{q^2}{2M} \right). \qquad (7)$$

Here y_M is the West scaling factor defining the nuclear Compton profile J_M of a nucleus of mass M, and $\hat{\mathbf{q}}$ is a unit vector along $\mathbf{q}$. The impulse approximation is exact at infinite q but for finite momentum transfers a number of refinements must be made to the data, mentioned in Sec. III of this work.

III. SAMPLE DESCRIPTION AND DATA ANALYSIS

A. Sample preparation

All samples were studied as powdered solids. NaH (99.99% purity) and SiGNa (34.6 wt% Na) were purchased from Sigma Aldrich. SiGNaH was prepared by the reaction of SiGNa with hydrogen gas in accordance with the literature.[18] SiGNa consists of particulate, amorphous Na metal dispersed in the nanoscale pores of the silica gel framework. Exposure to H_2 in the formation of SiGNaH does not damage the silica framework, with identifiable and isolated particles of crystalline NaH forming on the order of 20–50 nm.

Samples were stored and handled under an inert (argon) atmosphere. For the collection of neutron data, samples were placed in an airtight aluminum sample holder and cooled to 4 K.

B. VESUVIO data collection

VESUVIO is an inverse geometry, time of flight (ToF) spectrometer at the ISIS facility (Chilton, UK). The measured count-rate can be achieved by incorporating the impulse approximation into that of standard theory, and is given by[26]

$$C_m(t) = \left[\frac{E_0 I(E_0)}{q} \right] \sum_{M} A_M J_M(y_M) \otimes R_M(t). \qquad (8)$$

In the above equation $I(E_0)$ is the intensity of incident neutrons with energy E_0, A_M is the amplitude of scattering for each mass M and $R_M(t)$ is a resolution function in time for each mass. It is also assumed in the data analysis that $J_M(y_M)$ has a normalized Gaussian form

$$J_M(y_M) = \frac{1}{\sqrt{2\pi \omega_M^2}} \exp \left[\frac{-y_M^2}{2\omega_M^2} \right], \qquad (9)$$

where ω_M is the peak width in momentum space to be fitted along with A_M. For heavy atoms, calculations show that at temperatures comparable to the Debye temperature the momentum distribution is close to a Gaussian.[27] Non-Gaussian effects are important mainly for hydrogen and deuterium momentum distributions, for which the characteristic temperature corresponding to frequencies of vibration are usually much higher than the sample temperature. As part of the standard data fitting for NCS, non-Gaussian terms have been included for analysis of the hydrogen profile.[1,11,12] Also in accordance with standard practice, all raw forward scattering data collected in this work have undergone corrections for multiscattering, final-state effects, and for a gamma background signal. The backscattering signals have been corrected for multiscattering and the signal from the sample has been subtracted for each spectra.

C. Backscattering fitting technique

It has been stated that an NCS ToF spectrum consists of peaks arising from each atomic mass in the system. As atomic mass increases, peak positions become closer and a supposition of peaks results. This one peak then needs to
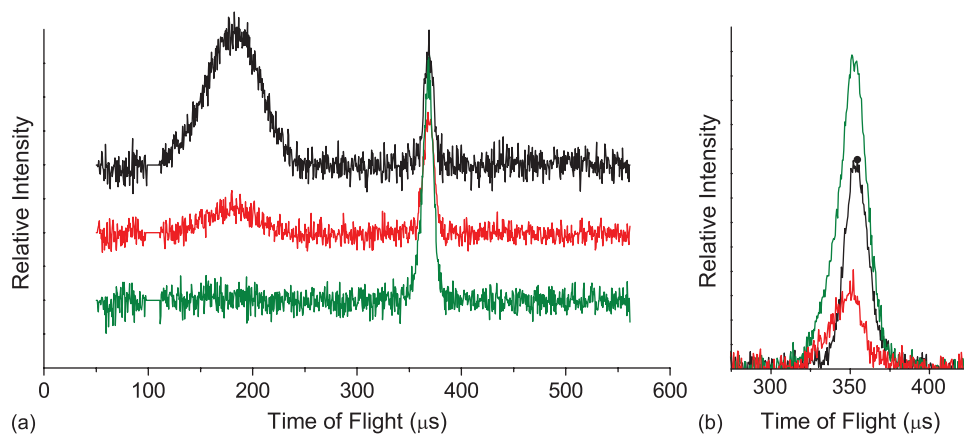
FIG. 1. Examples of forward (a) and back (b) scattered ToF data for NaH (black), SiGNaH (red), and SiGNa (green). Data plotted are for single banks of detectors on VESUVIO, with integrated proton currents of 2267.2, 2650.8, and 1941.8 μAh, respectively.

be separated into its constituent, single-mass peaks, and for each of those ω_M and A_M must be fitted. In systems, such as SiGNa and SiGNaH (and even NaH if the aluminum sample were fitted), where the heavier masses are not dissimilar this can be problematic.

In order to get around this fitting problem, we make use of the relationship

$$\frac{A_x}{A_y} = \frac{N_x \sigma_x}{N_y \sigma_y}, \qquad (10)$$

and thus if the stoichiometry of the sample is known (and therefore the atomic number densities, N_M), along with the total neutron scattering cross-sections for each atomic species, σ_M, a ratio of A_M values can be fixed. It has been stated that on VESUVIO all scattering is incoherent due to the short neutron wavelengths, which includes scattering from the coherent cross-section. This then allows subsequent fitting of ω_M values.

IV. RESULTS AND DISCUSSION

A. Forward scattering

Figure 1 shows the corrected neutron ToF spectra from the first of six forward scattering banks (a) and one of three backscattering banks (b) of detectors on VESUVIO for NaH, SiGNa, and SiGNaH. It is evident from the large peak at lower flight times in Fig. 1(a) for the NaH and SiGNaH spectra that there is scattering from H, whereas, as expected, there is a lack of such a feature in SiGNa. The other feature visible in Fig. 1(a) for all three spectra is a supposition of peaks from

O, Na, Si, and sample container (Al) species, and is the only feature present in the backscattering spectra of Fig. 1(b). This heavy-mass feature is not analyzed for forward scattering but is examined from the backscattering spectra as will be discussed later. It should be noted that contribution from the container is removed for the analysis of backscattering spectra. The region from 100 to 116 μs in Fig. 1(a) has been excluded as standard due to contamination from a second gold resonance in the detector setup.

Following methods outlined in Sec. III, the H peaks in the forward spectra have been fitted for NaH and SiGNaH over 47 detectors in the angular range $30° < 2\theta < 70°$, allowing determination of neutron Compton profiles and proton radial momentum distributions [$p^2 n(p)$]. These are plotted in Figs. 2 and 3, respectively. The widths of proton momentum distributions, along with average kinetic energies calculated from them are presented in Table I. It should be noted that the mean kinetic energy of 69.40 meV for NaH is similar to that given by Colognesi et al. from inelastic neutron scattering studies of the phonon density-of-states for NaH,[16] given as 66.39 meV at a slightly higher temperature of 20 K. It can be seen from Figs. 2 and 3 and Table I that the measured widths and momentum distributions are quite similar for both NaH and SiGNaH. Inelastic neutron spectroscopic measurements of these systems show no additional features in SiGNaH, despite particle sizes being of the order of 20–50 nm but there is slight discrepancy in features between 150–200 meV as seen in Ref. 18. It could thus be concluded that the neutron Compton profile for the proton in NaH(bulk) and SiGNaH would be similar, which as seen in Fig. 2 is indeed the case. The radial momentum distributions of the protons would be expected to

TABLE I. Summary of profile widths (Å^{-1}) and proton kinetic energies (meV) from NCS data.

System	H width	$\langle$ K.E. $\rangle_{proton}$	Na width	Si width	O width
NaH (bulk)	3.323 ± 0.015	69.40 ± 0.70	7.242 ± 0.365		
SiGNaH	3.280 ± 0.070	66.18 ± 3.49	6.263 ± 0.709	12.473 ± 2.954	11.045 ± 0.529
SiGNa			5.329 ± 0.243	12.250 ± 1.543	12.779 ± 0.284
NaH (INS, 20 K) (Ref. 16)		66.39			
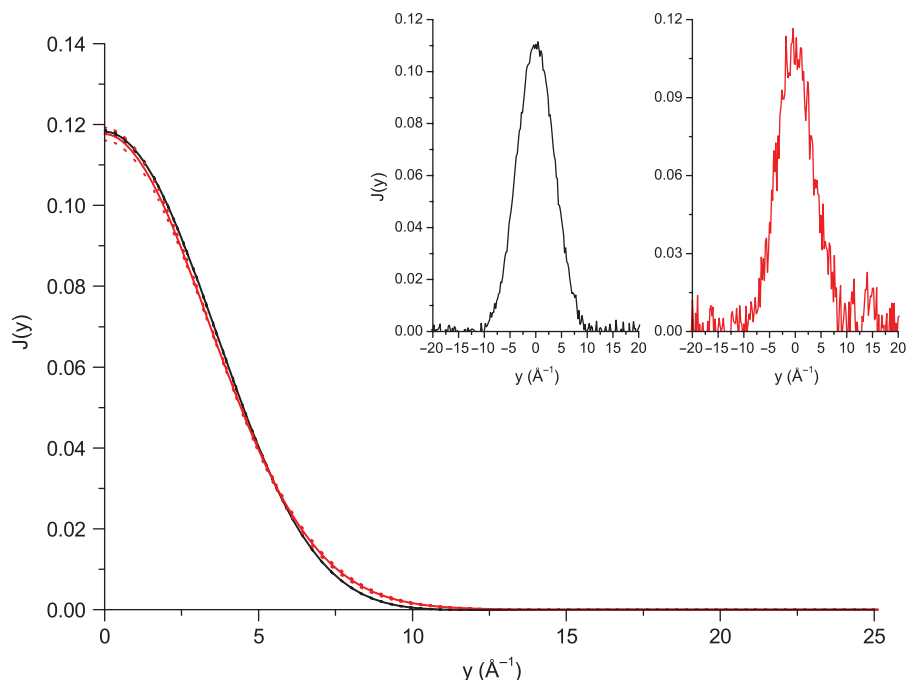
FIG. 2. Neutron Compton profile of NaH (black) and SiGNaH (red). Error limits are shown as dashed lines, but are too small to see at higher values for $J(y)$. Inset: Raw data in y-space.

emphasize any small differences in $J(y)$, and it can be seen from Fig. 3 that there is a shift in line shape to higher values of p. This difference is greater than experimental error but still slight, and could reflect a nanoscale confinement effect. However, due to the range of nanoparticle size distributions in SiGNaH it is not possible at this stage to state this with complete certainty, considering the extreme similarities in $J(y)$ and the fundamental peaks in the INS data.

B. Backscattering

As the scattering angle increases in NCS ToF spectra, there is an increase in the separation of peaks corresponding to different masses. For this reason, separation of the heavy-mass peak in Fig. 1 into those of its constituent masses
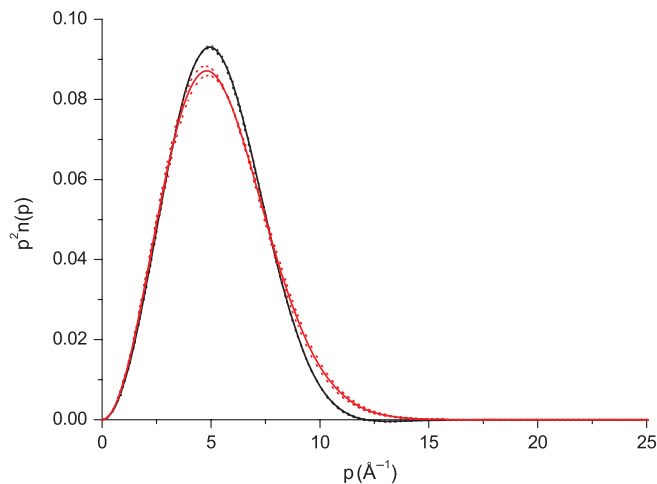
FIG. 3. Radial momentum distributions for NaH in bulk (black) and SiGNaH (red). Error limits are shown as dashed lines.

was undertaken by examining the spectra collected from 131 backscattering detectors for each system in the range $90°$ < 2θ < $160°$ (after subtraction of signal from the sample container). Figure 1(b) shows an example ToF spectrum for the first backscattering bank of VESUVIO.

As was outlined in Sec. III, the spectra were fitted for each individual mass, with widths being extracted and presented in Table I. Upon examination of the Na peaks it can be seen that the fitted width is lower in SiGNa than in NaH, with the value for SiGNaH laying approximately halfway between these two. The value of 5.427 $Å^{-1}$ for SiGNa is in agreement with widths extracted from elemental Na by Fulton *et al.* (approximately 5.8 $Å^{-1}$ at 30 K) on the VESUVIO predecessor, EVS, despite Na in SiGNa being in an amorphous state with possible increased ionic character near contacts with the silica framework.[28] One of the conclusions from Fulton *et al.* was that their study was not sensitive to phase-changes in Na, and thus it is little surprise that our result lies within their limits. It was also shown that the measured width increases with temperature and our value measured at 4 K is concordant with their extrapolated result.

A shift to higher value for the Na width in NaH is particularly important, however, in that it reflects the increased potential felt by the Na^+ nuclei in the ionic salt compared to the metallic state, something that may have been considered unlikely by the use of NCS due to the resolution of VESUVIO falling off with increased mass.

Of equal interest is the value for the Na profile width in SiGNaH falling approximately halfway between those of NaH and SiGNa. As detailed in the synthetic reference for SiGNaH, hydrogenation of the SiGNa precursor resulted in only half of the available Na being reacted to give NaH ($\sim54\%$), with the remaining still existing as amorphous Na in the gel. A value for Na width being approximately halfway

between the NaH and SiGNa values is thus a logical average of the two environments.

In order to evaluate whether the fixing of scattering amplitudes in the fitting routine yields chemically plausible results, the profile widths for Si and O are also presented alongside those for Na in Table I. The similarity in Si width in both gel samples, despite the larger errors for this heavier mass, reflects the unchanged Si environment from SiGNa to SiGNaH (where Si exists locally as tetrahedral SiO_4 units). The O nuclei are expected to be more sensitive to NCS, being lighter than their Na or Si counterparts and again similar values for profile widths result for SiGNa and SiGNaH. There is a slight increase in width in SiGNa, greater than experimental error, which would seem to support the idea that there is ionization of the amorphous Na at close contacts with the O surface of the silica gel. It must be noted, however, that there still exists amorphous Na in addition to NaH in the SiGNaH sample, and so any definite conclusion as to this ionization affecting the average O profile width cannot be drawn at this stage. However, in addition to the correlated changes in Na environment in NaH, SiGNa, and SiGNaH, the similarities in Si width and only slight differences in O width would seem to suggest that the fixing of amplitude ratio in the analysis of the backscattering data is a suitable technique to aid the fitting of multiple-mass peaks.

V. CONCLUSION

We have reported here the application of NCS to the study of bulk NaH in addition to that of NaH nanoparticles and amorphous Na encapsulated within silica gel (SiGNaH and SiGNa, respectively). We have shown that despite the presence of silica gel (an amorphous framework in itself) and a range of particle sizes in the nano-regime, NCS is able to analyze proton momentum distributions in NaH. Mean kinetic energies calculated from these widths are in agreement with previous inelastic neutron scattering studies, and it is seen that in SiGNaH there is a shift in proton radial momentum distributions to higher values of p compared to bulk NaH. Also reported are examinations of NCS profile widths for heavier masses in the systems. Knowing the stoichiometric ratio of these elements enables fitting of the backscattering spectra on VESUVIO, and we have shown that analysis of the three systems yields a correlated result for Na, whereby moving from the amorphous metallic state in SiGNa to the ionic state in NaH results in an increased profile width. The mixed state SiGNaH sample yields an intermediate profile width. Further support for these analyses is found in the Si and O widths for the gel samples.

[1] C. Andreani, D. Colognesi, J. Mayers, G. F. Reiter, and R. Senesi, Adv. Phys. **54**, 377 (2005).

[2] C. A. Chatzidimitriou-Dreisman, T. Abdul-Redah, and M. Krzystyniak, Phys. Rev. B **72**, 054123 (2005).

[3] C. A. Chatzidimitriou-Dreisman, T. Abdul Redah, R. M. F. Streffer, and J. Mayers, Phys. Rev. Lett. **79**, 28394 (1997).

[4] G. F. Reiter, C. Burnham, D. Homouz, P. M. Platzman, J. Mayers, T. Abdul-Redah, A. P. Moravsky, J. C. Li, C. K. Loong, and A. I. Kolesnikov, Phys. Rev. Lett. **97**, 247801 (2006).

[5] V. Garbuio, C. Andreani, S. Imberti, A. Pietropaolo, G. F. Reiter, R. Senesi, and M. A. Ricci, J. Chem. Phys. **127**, 154501 (2007).

[6] A. Fulton, R. A. Cowley, and A. C. Evans, J. Phys. Condens. Matter **6**, 2977 (1994).

[7] A. C. Evans, J. Mayers, and D. Timms, J. Phys. Condens. Matter **6**, 4197 (1994).

[8] A. Fielding, D. Timms, and J. Mayers, Europhys. Lett. **44**, 255 (1998).

[9] M. Krzystyniak, C. A. Chatzidimitriou-Dreisman, M. Lerch, Z. T. Lalowicz, and A. Szymocha, J. Chem. Phys. **126**, 124501 (2007).

[10] D. Colognesi, A. Pietropaolo, R. Senesi, and A. J. Ramirez-Cuesta, Phys. Rev. B **76**, 174206 (2004).

[11] G. F. Reiter, J. Mayers, and J. Noreland, Phys. Rev. B **65**, 104305 (2004).

[12] A. Pietropaolo, R. Senesi, C. Andreani, A. Botti, M. A. Ricci, and F. Bruni, Phys. Rev. Lett. **100**, 127802 (2008).

[13] S. E. Pagnotta, F. Bruni, R. Senesi, and A. Pietropaolo, Biophys. J. **96**, 1939 (2009).

[14] G. Reiter, R. Senesi, and J. Mayers, Phys. Rev. Lett. **105**, 148101 (2010).

[15] L. Kosidowski, A. V. Powell, and J. Mayers, Physica B **241**, 335 (1998).

[16] D. Colognesi, A. J. Ramirez-Cuesta, M. Zoppi, R. Senesi, and T. Abdul-Redah, Physica B **350**, e983 (2004).

[17] T. Abdul-Redah, P. A. Georgiev, D. K. Ross, M. Krzystyniak, and C. A. Chatzidimitriou-Dreisman, J. Alloys Compd. **404**, 787 (2005).

[18] A. Sartbaeva, S. A. Wells, M. Sommariva, M. J.T. Lodge, M. O. Jones, A. J. Ramirez-Cuesta, G. Li, and P. P. Edwards, J. Cluster Sci. **21**, 543 (2010).

[19] R. A. Cowley and J. Mayers, J. Phys. Condens. Matter **18**, 5291 (2006).

[20] T. Abdul-Redah and C. A. Chatzidimitriou-Dreisman, Physica B **350**, e1035 (2004).

[21] T. Abdul-Redah, P. A. Georgiev, D. K. Ross, M. Krzystyniak, C. A. Chatzidimitriou-Dreisman, Physica B **385**, 57 (2006).

[22] D. Homouz, G. F. Reiter, J. Eckert, J. Mayers, and R. Blinc, Phys. Rev. Lett **98**, 115502 (2007).

[23] J. Mayers, Phys. Rev. B **41**, 41 (1990).

[24] S. W. Lovesey, *Thermal Neutron Scattering from Condensed Matter* (Oxford University Press, Oxford, 1984).

[25] G. Squires, *Introduction to the Theory of Thermal Neutron Scattering* (Dover, New York, 1996).

[26] J. Mayers and T. Abdul-Redah, J. Phys. Condens. Matter **16**, 4811 (2004).

[27] J. Mayers, C. Andreani, and G. Baciocco, Phys. Rev. B **39**, 2022 (1989).

[28] M. Shatnawi, G. Paglia, J. L. Dye, K. Cram, M. Lefenfeld, and S. J. L. Billinge, J. Am. Chem. Soc. **129**, 1386 (2007).